Use of Multiple Gauges and Microwave Attenuation of Precipitation for Satellite Verification

EUNHO HA* AND GERALD R. NORTH

Climate System Research Program, Texas A&M University, College Station, Texas

(Manuscript received 10 May 1993, in final form 23 September 1993)

ABSTRACT

In this paper both a microwave attenuation measurement along a horizontal line and multiple point gauge measurements are analyzed as possible ground-truth designs to validate satellite precipitation retrieval algorithms at the field of view spatial level (typically about 20 km). The design consists of comparing a sequence of pairs of contemporaneous measurements taken from the ground and from space. The authors examine theoretically the variance of expected differences between the two systems. The line average measurement leads to a smaller mean-square error compared to the case of a single point gauge, since some of the small-scale variability of the rain field is smoothed away by the line integration. The multiple point gauge measurements also give smaller mean-square error than that of a single point gauge. The centroid of the line and point gauge configurations are considered to be located randomly inside the field of view for different overpasses. A space–time spectral formalism is used with a noise-forced diffusive rain field to find the mean-square error. By considering instantaneous ground and satellite measurement pairs over about 50 visits when raining, we can reduce the expected error to approximately 10% of the standard deviation of climatological variability. This is considered to be a useful level of tolerance for identifying biases in the retrieval algorithms. It is found that the multiple point gauges (especially two gauges) are the economical ground-truth design compared to the microwave attenuation based on the mean-square error comparison. The major finding of this study is that a significant improvement over the point gauge is obtained by adding a single additional piece of information; adding more gauges or extending the line of attenuation is not an important improvement.

1. Introduction

Ground truthing is a major problem in the satellite estimation of rain rate. The main problem is that the measurement taken by the satellite sensor is fundamentally different from the one it is to be compared with on the ground. This is because the ideal satellite measurement is of an area average over the field of view (FOV) of the instrument footprint, while the ground measurement is inevitably over a lower dimension such as a point or line. Back-scattered radar may make the problem simpler, since it could be used to estimate (horizontal) area averages. Unfortunately, the algorithms for radar backscatter estimation of rain rate are controversial at best. Hence, we turn here to multiple point gauges and line averages.

It has been suggested that the microwave attenuation is a better estimate of average rain rate along the line of attenuation, since it is insensitive to drop size distribution (Atlas and Ulbrich 1977). While the area average satellite estimate is still different from the line average, the latter may offer some advantage over a comparison with a point gauge, since a line segment is more representative of the FOV than a point. North et al. 1994 give an examination of the problem for a single point gauge. In the present paper we examine the expected error characteristics for the line average measurement as well as the multiple point gauge measurements inside an FOV. We do not consider the errors inherent in the individual instruments, but rather take them to be ideal. Random instrument errors will make the difference variance larger, while biases will lead to an offset of the distribution mean from zero.

Our problem may be stated as follows: we collect a series of single FOV measurements over a period of time. Somewhere in the FOV during each visit a ground measurement (line attenuation measurement or multiple point gauge measurement in our study) is taken coincidentally with each satellite overpass. The location of the centroid of the FOV with respect to the position of the ground measurement device will vary randomly (uniformly distributed in a space) from one visit to another. The difference between the ground measurement and the perfect satellite measurement will differ

* Current affiliation: Department of Statistics, Enje University, Pusan, Republic of Korea.

Corresponding author address: Dr. Gerald North, Climate System Research Program, Texas A&M University, College Station, TX 77843-3150.

randomly with zero mean from visit to visit, since ideally one is an unbiased estimator of the other. We may form a distribution of the differences for a number of visits, say N. We seek the standard deviation of this histogram. For the technique to be useful, the standard deviation must be comparable to or less than the size of biases in the satellite rain-rate algorithm we are trying to test. In the most interesting cases the correlation of rain rate for the area average over a single FOV from one visit to another is negligible; hence, we can consider the N visits as independent estimates. The error variance is then expected to be inversely proportional to N.

Strictly speaking, one should expect a bimodal distribution of error: the first peak being a very narrow one centered at zero corresponding to no rain being observed in either system, and the second peak corresponding to the raining events. We should throw out the no-rain events and keep only those in which rain is (thought to be) occurring in the FOV. Hence, N is to be reduced to the number of visits in which rain is suspected within the FOV. While this is still not a wholly satisfactory solution to the problem, we consider it a useful starting point for the analysis, which allows for great simplification in the calculation.

Formally, we consider two measurements taken from the nth visit, the satellite measurement Ψ_s^n and a ground measurement Ψ_g^n. If we use the mean-square error as an index of our accuracy in estimating the ground measurement by satellite measurement, the mean-square error is

$$\epsilon_1^2 = \langle (\Psi_s^n - \Psi_g^n)^2 \rangle, \tag{1}$$

where the ensemble mean includes all the possible realizations of the rain-rate field along with all the uniformly distributed locations of the centroid of the FOV holding the ground configuration fixed. If, as argued above, the members of the sequence of pairs of measurements are statistically independent [autocorrelation times for a typical area the size of an FOV are only an hour or so, whereas revisit intervals for a satellite are an order of magnitude longer; e.g., Bell et al. (1990)], then the average mean-square error for N visits is

$$\epsilon_N^2 = \frac{\epsilon_1^2}{N}. \tag{2}$$

As we can see from (2), the advantage of this strategy is that we can easily add new measurements and thus we can make the error as small as we want it to be (i.e., by taking N sufficiently large). North et al. (1994) applied this simple strategy with a single-point gauge measurement as the ground system. They found that it leads to a satisfactorily (approximately 10% of climatological variation) narrow histogram provided the rain rates are averaged over a few minutes and the averaging is over about 60 visits. This time averaging of a few minutes is thought to mimic the fact that the satellite actually measures a vertical average of the rain rate and the rain is expected to take from 2 to 7 min to fall out of the column.

In this study we consider a microwave attenuation measurement and multiple point gauge measurements separately as the ground-truth designs. We expect that the line average of the microwave attenuation measurements will reduce the small-scale variability much as the time average does for a point gauge measurement. Such averaging along the line should make the result less dependent upon the specific rain field model chosen for the calculations than that of raingage design. We also expect that the average of multiple point gauge measurements will reduce the small-scale variability and thus will lead to a smaller mean-square error. In this paper, we consider a random field $\psi(\mathbf{r}, t)$ defined in the $\mathbf{r} = (x, y)$ plane and along the time axis t. Let the ensemble average of $\psi(\mathbf{r}, t)$ be zero and its variance at a point in space and time be σ^2. We assume that the random field is homogeneous in space and time. This assumption amounts to the statement that the lagged covariance is a function only of $|\xi|$ and $|\tau|$, where $\xi = \mathbf{r} - \mathbf{r}'$ and $\tau = t - t'$. We denote the lagged covariance by

$$\langle \psi(\mathbf{r}, t)\psi(\mathbf{r}', t) \rangle = \sigma^2 \rho(\xi, \tau), \tag{3}$$

where the angle brackets denote the ensemble average and $\rho(\xi, \tau)$ is the space–time lagged autocorrelation function with $\rho(0, 0) = 1$. Most of what follows can be expressed in terms of the Fourier representations of the space–time fields. We define the normalized wavenumber–frequency spectrum of the space–time field by the Fourier transformation of the autocorrelation

$$S(\nu, f) = \iiint \rho(\xi, \tau) \exp[2\pi i(\xi \cdot \nu + f\tau)] d^2\xi d\tau, \tag{4}$$

where the integrals run over all space.

We derive a mean-square error in terms of a spectral density representation that was derived by North and Nakamoto (1989, hereafter referred to as NN). The NN formalism has proven especially useful in the satellite sampling error problems (North et al. 1991; North et al. 1993). In this paper we compute the expected mean-square error for a few numerical examples that are likely to be useful in actual ground-truth programs.

2. Ground-based microwave attenuation of precipitation

In this section, we derive the mean-square error of the difference between the line average and the satellite FOV average. We first provide the mean-square error for instantaneous rain rate and then examine the mean-square error for a short time-averaged rain rate.

For a line within FOVs, the line average of instantaneous rain rate is defined by

$$\Psi_l = \frac{1}{l}\int_{\mathbf{r}_s}^{\mathbf{r}_e} \psi(\mathbf{r}, t)ds, \tag{5}$$

where l is the length of a line, $\mathbf{r}_s = (x_s, y_s)$ is the starting point, and $\mathbf{r}_e = (x_e, y_e) = (x_s + l, y_s)$ is the end point of a line; $ds \equiv |d\mathbf{r}|$. Note that the line average (5) can be written

$$\Psi_l = \frac{1}{l}\int_{x_1}^{x_1+l} \psi(x, y_1, t)dx. \tag{6}$$

Now consider the satellite estimation of the line average in (5). The satellite passes over the site and some (e.g., one or two in our study) of the FOVs in the swath along the ground track cover the line. The satellite FOVs are usually elliptical with fuzzy edges. We approximate FOVs by contiguous rectangles aligned parallel with the microwave link and raingages to avoid mathematical complications coming along with the typical FOVs. We denote the rectangular FOV having area $A = ab$ by R_k and it is given by

$$R_k = \left[-\frac{a}{2} + (k-1)a, \frac{a}{2} + (k-1)a\right] \otimes \left(-\frac{b}{2}, \frac{b}{2}\right) \qquad k = 1, 2, \cdots.$$

In most cases, the line length is less than the width of an FOV and thus the FOVs of interest are R_1 and R_2. Figure 1 shows the possible locations of a line schematically.

Since the centroid of the FOV is located randomly with respect to the position of the line (i.e., to the position of $\mathbf{r}_1$) for each visit, we can take the centroid to be fixed and thus consider $\mathbf{r}_s$ to be randomly located within an FOV R_1. Therefore, we have a uniform distribution as a probability distribution of $\mathbf{r}_s$:

$$P(\mathbf{r}_s) = \begin{cases} \dfrac{1}{A}, & \text{when} \quad \mathbf{r}_s \in R_1 \\ 0, & \text{otherwise.} \end{cases} \tag{7}$$

We may form the satellite estimation for the ground truth Ψ_l:

$$\Psi_s = \frac{1}{2A}\left[\int_{R_1} \psi(\mathbf{r}, t)d^2\mathbf{r} + \int_{R_k} \psi(\mathbf{r}, t)d^2\mathbf{r}\right] \quad k = 1, 2, \tag{8}$$

where R_1 is the FOV that covers $\mathbf{r}_s$ and R_k is the FOV that covers $\mathbf{r}_e$. Note that when FOV R_1 covers a whole line, the satellite estimate becomes

$$\Psi_s = \frac{1}{A}\int_{R_1} \psi(\mathbf{r}, t)d^2\mathbf{r}. \tag{9}$$

Since $\mathbf{r}_s$ is uniformly distributed, the probability of using only FOV R_1 is $p_1 = (a - l)/a$ and using both R_1 and R_2 is $p_2 = l/a$ as satellite estimation. Thus, the expected area of FOV in satellite estimation becomes $ab + bl$. We use the mean-square error as the measure of our accuracy in estimating the line measurement Ψ_l by the satellite measurement Ψ_s. The mean-square error for a single visit is defined as

$$\epsilon_1^2 = \langle(\Psi_l - \Psi_s)^2\rangle. \tag{10}$$

By inserting the space–time Fourier transform of $\psi(\mathbf{r}, t)$ into the error formula (see NN for more detail), we can derive the mean-square error

$$\epsilon_1^2 = \sigma^2 \iint S(\nu)|H(\nu)|^2 d^2\nu, \tag{11}$$

where

$$S(\nu) = \int S(\nu, f)df \tag{12}$$

is the contemporaneous spatial spectral density of the field and $H(\nu)$ is a design filter function. For the satellite estimation of the line average, the design filter function becomes

$$|H(\nu)|^2 = \begin{cases} |H_1(\nu)|^2, & \text{when} \quad \mathbf{r}_e \in R_1, \\ |H_2(\nu)|^2, & \text{when} \quad \mathbf{r}_e \in R_2, \end{cases} \tag{13}$$

where

$$|H_k(\nu)|^2 = G^2(\pi l\nu_x) + G^2(\pi a\nu_x)G^2(\pi b\nu_y)\cos^2[\pi(k-1)a\nu_x] - 2G(\pi l\nu_x)G(\pi a\nu_x)G(\pi b\nu_y)\cos[2\pi\mathbf{r}_s\nu + \pi l\nu_x - \pi(k-1)a\nu_x]\cos[\pi(k-1)a\nu_x], \tag{14}$$

$k = 1, 2$, and $G(\pi x) \equiv \sin(\pi x)/\pi x$. The function $G(\pi x)$ is known as the sinc function in physical optics and the Bartlett kernel in time series analysis (Blackman and Tukey 1959). Due to the random location of the line, we need the expectation value of the mean-square error with respect to all possible locations of a line. Using the uniform distribution of $\mathbf{r}_s$, one can compute the following formula:

$$E[\cos(2\pi\mathbf{r}_s\nu)] = \begin{cases} p_1G[\pi(a-l)\nu_x]G(\pi b\nu_y)\cos(\pi l\nu_x), & \text{when} \quad \mathbf{r}_e \in R_1, \\ p_2G(\pi l\nu_x)G(\pi b\nu_y)\cos[\pi(a-l)\nu_x], & \text{when} \quad \mathbf{r}_e \in R_2, \end{cases} \tag{15}$$

$$E[\sin(2\pi\mathbf{r}_s\nu)] = \begin{cases} -p_1G[\pi(a-l)\nu_x]G(\pi b\nu_y)\sin(\pi l\nu_x), & \text{when} \quad \mathbf{r}_e \in R_1, \\ p_2G(\pi l\nu_x)G(\pi b\nu_y)\sin[\pi(a-l)\nu_x], & \text{when} \quad \mathbf{r}_e \in R_2, \end{cases} \tag{16}$$

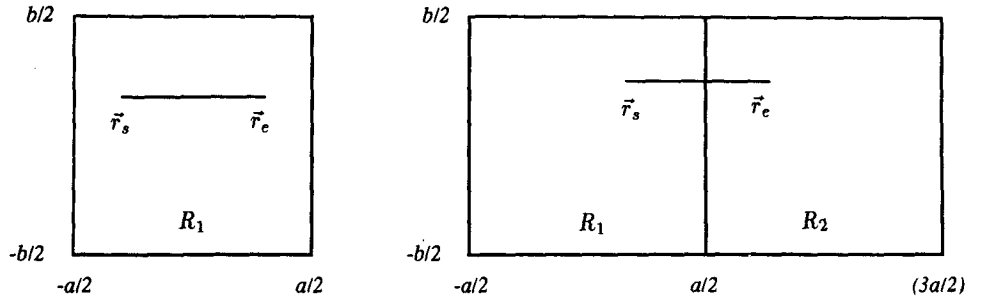

FIG. 1. Two possible locations of a line where a starting point is located within R_1.

where $p_1 = (a - l)/a$ and $p_2 = l/a$. Applying some familiar trigonometric identities to the formulas (15) and (16), we can obtain the expected mean-square error

$$E_1^2 = E(\epsilon_1^2) = \sigma^2 \iint S(\nu)|H_E(\nu)|^2 d^2\nu, \tag{17}$$

where

$$|H_E(\nu)|^2 = E[|H(\nu)|^2] = \int_{\mathbf{r}_e \in R_1} P(\mathbf{r}_s)|H_1(\nu)|^2 d\mathbf{r}_s + \int_{\mathbf{r}_e \in R_2} P(\mathbf{r}_s)|H_2(\nu)|^2 d\mathbf{r}_s$$
$$= G^2(\pi l\nu_x) + G^2(\pi a\nu_x)G^2(\pi b\nu_y)[p_1 + p_2 \cos^2(\pi a\nu_x) - 2\cos(\pi l\nu_x)G(\pi l\nu_x)]. \tag{18}$$

Note that for a point gauge measurement ($l \to 0$), the expected mean-square error becomes

$$E_1^2 = \sigma^2 \iint S(\nu)[1 - G^2(\pi a\nu_x)G^2(\pi b\nu_y)]d^2\nu, \tag{19}$$

which is equivalent to the formula derived in North et al. (1993b). For comparative purposes, we introduce the dimensionless error variance

$$V_1^2 = \frac{E_1^2}{\sigma_A^2}, \tag{20}$$

where σ_A^2 is the climatological variance of one FOV average and it may be written in the spectral density representation

$$\sigma_A^2 = \sigma^2 \iint S(\nu)G^2(\pi a\nu_x)G^2(\pi b\nu_y)d^2\nu. \tag{21}$$

Next we consider a short time average of the line measurement and satellite measurement. In practice, the satellite measures the column average of rain rate, which is equivalent to a time average of a few minutes at the surface. In this case the line measurement and the satellite estimation over an interval T for a visit are formed

$$\Psi_{lT} = \frac{1}{lT}\int_{-T/2}^{T/2}\int_{x_s}^{x_s+l} \psi(x, y_s, t)dxdt = \frac{1}{T}\int_{-T/2}^{T/2} \Psi_l dt, \tag{22}$$

$$\Psi_{sT} = \frac{1}{2AT}\int_{-T/2}^{T/2}\left[\int_{R_1} \psi(\mathbf{r}, t)d^2\mathbf{r} + \int_{R_k} \psi(\mathbf{r}, t)d^2\mathbf{r}\right]dt$$
$$= \frac{1}{T}\int_{-T/2}^{T/2} \Psi_s dt, \tag{23}$$

where the subscript of Ψ_{lT} and Ψ_{sT} indicates the time average of the line and satellite measurement, respectively. We then form the mean-square error

$$\epsilon_{1T}^2 = \langle(\Psi_{lT} - \Psi_{sT})^2\rangle, \tag{24}$$

which can be obtained as

$$\epsilon_{1T}^2 = \sigma^2 \iint S_T(\nu)|H(\nu)|^2 d^2\nu, \tag{25}$$

where

$$S_T(\nu) = \int G^2(\pi Tf)S(\nu, f)df \tag{26}$$

and the design filter is given by (14). Thus we have the expected mean-square error

$$E_{1T}^2 = E(\epsilon_{1T}^2) = \sigma^2 \iint S_T(\nu)|H_E(\nu)|^2 d^2\nu, \tag{27}$$

where $|H_E(\nu)|^2$ is in (18). The dimensionless error variance for the time-average case is then

$$V_{1T}^2 = \frac{E_{1T}^2}{\sigma_A^2}. \tag{28}$$

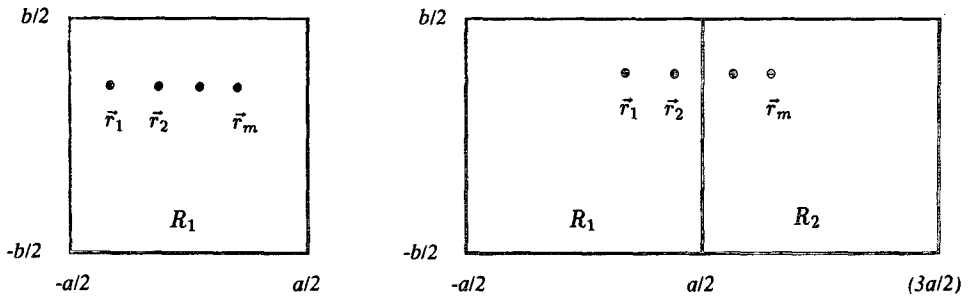

FIG. 2. Two possible locations of multiple point gauges where the first gauge is located within R_1.

3. Multiple point gauges

Let the point gauges be located within FOVs at

$$\mathbf{r}_j = (x_j, y_j) = [x_1 + (j-1)\Delta x, y_1] \qquad j = 1, 2, \cdots, m, \quad (29)$$

where $\Delta x = l/(m-1)$ and l is the distance between the first gauge $\mathbf{r}_1$ and the last gauge $\mathbf{r}_m$. Note that the distance between any two adjacent gauges is equal and is Δx. We can form the ground truth with m point gauge measurements:

$$\Psi_m = \frac{1}{m}\sum_{j=1}^{m} \psi(\mathbf{r}_j, t). \quad (30)$$

In our study, we assume that l is less than or equal to the width of an FOV, and thus, it is enough to consider two FOVs, namely, R_1 and R_2, for satellite estimation. Figure 2 shows the possible locations of m point gauges schematically.

Since the multiple point gauges problem is analogous to the line average problem, we adopt the same notation used in section 2. The satellite estimation for the ground truth defined in (30) is

$$\Psi_s = \frac{1}{2A}\left[\int_{R_1} \psi(\mathbb{r}, t)d^2\mathbb{r} + \int_{R_k} \psi(\mathbb{r}, t)d^2\mathbb{r}\right] \qquad k = 1, 2, \quad (31)$$

where R_1 is the FOV that covers $\mathbf{r}_1$ and R_k is the FOV that covers $\mathbb{r}_m$. Following the same procedure in section 2, we can compute the mean-square error of estimating the multiple point gauge measurements Ψ_m by the satellite measurement Ψ_s:

$$\epsilon_1^2 = \sigma^2 \iint S(\nu)|H(\nu)|^2 d^2\nu, \quad (32)$$

where

$$|H(\nu)|^2 = \begin{cases} |H_1(\nu)|^2, & \text{when } \mathbb{r}_m \in R_1, \\ |H_2(\nu)|^2, & \text{when } \mathbb{r}_m \in R_2, \end{cases} \quad (33)$$

and

$$|H_k(\nu)|^2 = G^2(\pi a\nu_x)G^2(\pi b\nu_y)\cos^2[\pi(k-1)a\nu_x] + \frac{1}{m^2}\sum_{p=1}^{m}\sum_{q=1}^{m}\exp[-2\pi i(\mathbb{r}_p - r_q)\cdot\mathbb{v}]$$
$$- \frac{2}{m}G(\pi a\nu_x)G(\pi b\nu_y)\sum_{p=1}^{m}\cos[\pi(k-1)a\nu_x]\cos[2\pi\mathbb{r}_p\nu - \pi(k-1)a\nu_x]. \quad (34)$$

Noting that $\mathbf{r}_1$ and $\mathbb{r}_m$ correspond to $\mathbf{r}_s$ and $\mathbf{r}_e$, respectively, in section 2, we can use the formulas (15) and (16) to compute the expected mean-square error:

$$E_1^2 = E(\epsilon_1^2) = \sigma^2 \iint S(\nu)|H_E(\nu)|^2 d^2\nu, \quad (35)$$

where

$$|H_E(\nu)|^2 = G^2(\pi a\nu_x)G^2(\pi b\nu_y)[p_1 + p_2\cos^2(\pi a\nu_x)] + \frac{G^2(\pi m\Delta x)}{G^2(\pi\Delta x)}$$
$$- \frac{2}{m}G^2(\pi a\nu_x)G^2(\pi b\nu_y)\cos(\pi l\nu_x)\sum_{j=1}^{m}\cos[2\pi(j-1)\Delta x\nu_x - \pi l\nu_x]. \quad (36)$$

For the two point gauges, we have

$$|H_E(\nu)|^2 = \cos^2(\pi l\nu_x) + G^2(\pi a\nu_x)G^2(\pi b\nu_y) \times [p_1 + p_2\cos^2(\pi a\nu_x) - 2\cos^2(\pi l\nu_x)]. \quad (37)$$

Note that as $m \to \infty$, the expected mean-square error becomes that of the line average in (18). For instantaneous measurement of a finite point gauge, the expected mean-square error diverges for the specific rainfield model chosen for numerical analysis; the same problem happens with a single point gauge design [see North et al. (1994) for more detail]. We found in section 2 that we can remove this problem with the continuous line average of the microwave attenuation measurement. Another way of avoiding the divergence problem is to use the short time average of rain rate. We can form a short time average of the multiple gauge measurements and satellite measurement

$$\Psi_{mT} = \frac{1}{T}\int_{-T/2}^{T/2} \Psi_m dt, \quad (38)$$

$$\Psi_{sT} = \frac{1}{T}\int_{-T/2}^{T/2} \Psi_s dt, \quad (39)$$

where the subscript of Ψ_{mT} and Ψ_{sT} indicates the time average of the multiple gauges and satellite measurement, respectively. We can derive the expected mean-square error

$$E_{1T}^2 = E(\epsilon_{1T}^2) = \sigma^2 \int\int S_T(\nu)|H_E(\nu)|^2 d^2\nu, \quad (40)$$

where

$$S_T(\nu) = \int G^2(\pi Tf)S(\nu, f)df \quad (41)$$

and the design filter $|H_E(\nu)|^2$ is in (36). The dimensionless error variance for the time-average case is then

$$V_{1T}^2 = \frac{E_{1T}^2}{\sigma_A^2}. \quad (42)$$

We can compute the dimensionless error variance by numerical double integration.

4. Numerical examples

To proceed, we need a spectrum for the rain field model that captures the main features of the space-time correlations of the rain-rate fluctuations. Fortunately, a simple model has been developed and it is reasonably accurate in describing the GATE (GARP) data that were taken over the tropical Atlantic in the summer of 1974 (Huddlow and Patterson 1979; Nakamoto et al. 1990). The model is a so-called noise-forced diffusive rain model and is defined by its governing equation

$$\tau_0 \frac{\partial\psi}{\partial t} - \lambda_0^2\nabla^2\psi + \psi = F(\mathbf{r}, t), \quad (43)$$

where τ_0 is a timescale for the rainfall process and λ_0 is a length scale, both inherent to the field. The forcing function F might be a white noise process in space and time but cutoff at some high wavenumber ν_c to prevent divergences (for pure white noise forcing the model has infinite point variance; see NN). The spectral density function found in NN is

$$S(\nu, f) = \frac{\alpha}{4\pi^2\tau_0^2 f^2 + (1 + 4\pi^2\lambda_0^2\nu^2)^2}, \quad (44)$$

where

$$\alpha = \frac{8\pi\tau_0\lambda_0^2}{\ln(1 + 4\pi^2\lambda_0^2\nu_c^2)^2}$$

is a normalization factor such that $\rho(0, 0) = 1$. For the GATE data of precipitation, these τ_0 and λ_0 take values around 12 h and 40 km, respectively (see NN).

Note that for the noise-forced diffusive rain model

$$S(\nu) = \int_{-\infty}^{\infty} S(\nu, f)df = \frac{\alpha}{2\tau_0(1 + 4\pi^2\lambda_0^2\nu^2)}, \quad (45)$$

$$S_T(\nu) = \frac{\alpha}{T^2}\left[\frac{T}{(1 + 4\pi^2\lambda_0^2\nu^2)^2} + \frac{\tau_0}{(1 + 4\pi^2\lambda_0^2\nu^2)^3} \times \left\{\exp\left[-\frac{T}{\tau_0}(1 + 4\pi^2\lambda_0^2\nu^2)\right] - 1\right\}\right]. \quad (46)$$

With $S(\nu)$ and $S_T(\nu)$, we can apply the formula in section 2 to compute numerical results of the dimensionless error variance for instantaneous and time average rainfall measurement. The 20-km × 20-km rectangular FOV, which is typical, is used for the numerical examples. We first present the DRMSE (dimensionless root-mean-square error), which is the square root of the dimensionless error variance (V_1^2) for an instantaneous measurement in Table 1. The line average removes the divergence problem that occurred in the case of point gauge measurement ($l \to 0$) [see North et al. (1994) for details]. We additionally can see from Table 1 that DRMSE, $V_1 = \text{rmse}/\sigma_A$, decreases as the length of line l increases. Since the DRMSE of an instantaneous measurement is finite and even small for a single visit, we can sharpen the histogram of the differences between the satellite measurement and the line measurement by adding independent measurements of several visits. The DRMSE of 60 visits, which is roughly equivalent to considering a month-long sampling period because the revisit interval is about 12 h, is also given by Table 1. We remind the reader that it may be more appropriate to consider N as pertaining only to raining FOVs. This will considerably reduce the effective number of visits so that an effective value of 60 may take as long as a year.

TABLE 1. The dimensionless root-mean-square error for noise-forced diffusive precipitation model tuned to GATE for a few-kilometer line average of instantaneous measurement: comparing the line average with rectangular 20-km × 20-km FOV. The rmse is normalized to the standard deviation of FOV average fluctations (climatology).

Line length l	DRMSE V_1	DRMSE with one month (V_{60})
0	∞	∞
2	1.315	0.170
4	1.150	0.148
6	1.043	0.135
8	0.963	0.124
10	0.902	0.116
12	0.852	0.110
14	0.813	0.105
16	0.781	0.101
18	0.756	0.098
20	0.735	0.095

TABLE 2. The dimensionless-root-mean-square error for noise-forced diffusive precipitation model tuned to GATE for several minutes averaging. Comparing the line averages with rectangular 20-km × 20-km FOV for a single visit. The rmse is normalized to the standard deviation of FOV average fluctuations (climatology).

T	$l = 0$ V_{1T}	$l = 10$ V_{1T}	$l = 20$ V_{1T}
0	∞	0.902	0.735
1	1.123	0.814	0.681
2	1.030	0.779	0.659
3	0.972	0.753	0.643
4	0.930	0.732	0.629
5	0.896	0.714	0.618
6	0.868	0.698	0.607
7	0.844	0.683	0.598
8	0.823	0.670	0.589
9	0.805	0.658	0.581
10	0.788	0.647	0.574

As discussed in the introduction, the DRMSE of N independent visits is obtained by

$$V_N = \frac{V_1}{N^{1/2}}. \tag{47}$$

Next we can examine the effect of time averaging in Table 2. The time averages range from 1 to 10 min for a rectangular FOV. We have seen that time averaging is essential to avoid the divergence problem of point gauge measurements ($l \to 0$) for the rain field model used in the numerical example. Time averaging reduces the DRMSE for all line lengths, and the amount of reduction for small length is larger than that of large length.

Figure 3 shows the DRMSE of multiple gauges and line average measurement for 10-min-averaging rain-rate measurement as a function of the distance l. The multiple point gauge and line measurement reduces the DRMSE compared to that of one point gauge for a single visit. It seems at first glance that Fig. 3 gives a paradoxical result because two gauges give smaller DRMSE than that of multiple point gauges and line average measurement where l is not too large. However, it is true only when the FOV size is smaller than the characteristic length scale of the field, which is 40 km (typical size of FOV is about 20 km × 20 km). We can explain the result of Fig. 3 by considering the variance of sample average. Note that one important factor determining the mean-square error is the variance of the average of the point gauge measurements. When samples are positively correlated, the variance of the average will generally be greater than that of a smaller number of independent samples (Jones 1975; Newton 1988, 161–163). We present Fig. 4, which uses a 200-km × 200-km FOV even though it is not a practical FOV size for better understanding of Fig. 3. Consider the two gauges that are located at (x_1, y_1) and $(x_1 + l, y_1)$ and three gauges that are located at (x_1, y_1), $(x_1 + l/2, y_1)$, and $(x_1 + l, y_1)$. For Fig. 4, when l is small (say $l < 20$), two gauge measurements are almost independent, but three gauge measurements are not independent. Thus, the average of three gauge measurements leads greater variance than that of two gauges. However, if l is large, three gauge measurements are also independent and thus it gives smaller variance than that of two gauges. Since the FOV size is not large (typically it is 20 km × 20 km), we can see from Fig. 3 that microwave attenuation and several raingage measurements for ground-truth purposes are a waste of money. Thus two gauges, if they are not too closely

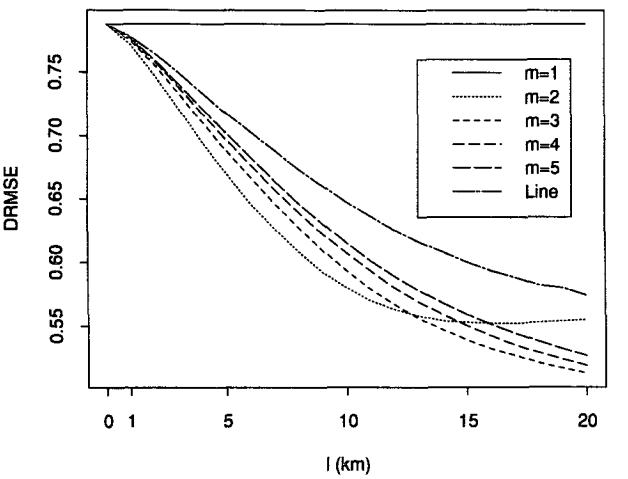

FIG. 3. The dimensionless root-mean-square error as a function of the distance l for 10-min averaging of rain rate with rectangular 20-km × 20-km FOV. Note that the rms is normalized to the standard deviation of FOV average fluctuations (climatology). The point gauges and line average measurement are used as the ground truth.

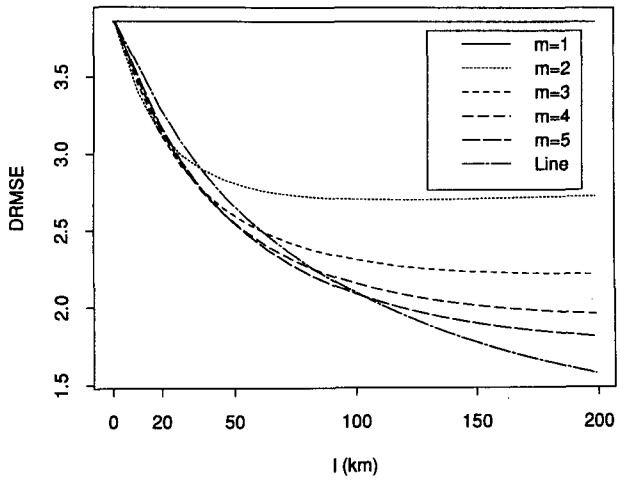

FIG. 4. The dimensionless root-mean-square error as a function of the distance l for 10-min averaging of rain rate with rectangular 200-km × 200-km FOV. Note that the rmse is normalized to the standard deviation of FOV average fluctuations (climatology). The point gauges and line average measurement are used as the ground truth.

located, appear to be the most economical ground-truth design.

5. Conclusions

In this paper we have seen that it is practical to compare line average measurements and/or multiple point measurements of instantaneous rain rate with those made for an individual field of view of a microwave radiometer onboard a satellite. The line measurements reduce the small-scale variability in the rain field much as the temporal smoothing does for a point gauge. A single pair of measurements is likely to contain a large component of random error due to the difference between a line or multiple points and an area average measurement. However, when about 60 measurement pairs (when raining) are aggregated, the rmse reduces to about 10% (of the climatological standard deviation). This appears to be small enough to allow the technique to be used for identification of biases in the retrieval algorithms for individual FOVs. It was shown that the (few minutes) temporal smoothing for line measurements also reduces the dimensionless rmse. Thus, when we use the time average and the line average together, we may need a smaller number of visits compared to the time average of point gauge measurements. We also found that use of more than one point gauge reduces the expected mean-square error, and this can be used advantageously to reduce error variance.

The evaluation of the difference between ground truth and areal average is based upon a mean-square error formalism. The spectral representation (North and Nakamoto 1989) was used to derive the mean-square error. The numerical analysis was carried out with a noise-forced diffusive rain model tuned to GATE data. This simplified model and its dependence on tuning to the GATE data represent shortcomings to our calculations. On the other hand, this approach is a reasonably good one for setting up the problem and carrying it through to see what factors are important.

At the same time we must recognize that the approach has a severe limitation, in that real rain is patchy; that is, its probability distribution has a large nonzero contribution at zero rain rate (delta function). Hence, many of the visits will lead to (no-rain, no-rain) measurements or perhaps (no-rain, rain) measurements where the second entry is the FOV average. This should lead to a sharp peak at zero in the histogram and a continuum for positive values of difference squared. A better measure of the error would come from throwing out (stratifying) all the nonraining events (say for the FOV average) and considering only the raining events. The mean-square error formalism adopted here is probably not the best for such an analysis. Similarly, we should adopt a model that has the appropriate probability distribution such as that devised by Bell (Bell et al. 1990). We are presently looking into such possibilities.

Acknowledgments. The authors wish to thank NASA through the TRMM Research Program. We also thank J. Valdés for helpful discussions.

REFERENCES

Atlas, D., and C. W. Ulbrich, 1977: Path- and area-integrated rainfall measurement by microwave attenuation in the 1–3 cm band. *J. Appl. Meteor.*, **17,** 1322–1331.

Bell, T. L., A. Abdullah, R. L. Martin, G. R. North, 1990: Sampling error for satellite-derived tropical rainfall: Monte Carlo study using a space–time stochastic model. *J. Geophys. Res.*, **95,** 2195–2205.

Blackman, R. B., and J. W. Tukey, 1959: *The Measurement of Power Spectra.* Dover Publications, 190 pp.

Hudlow, M., and V. Paterson, 1979: *GATE Radar Rainfall Atlas.* NOAA Special Rep. Government Printing Office, Washington, DC 158 pp.

Jones, R. H., 1975: Estimating the variance of time averages. *J. Appl. Meteor.*, **14,** 159–163.

Nakamoto, S., J. B. Valdes, and G. R. North, 1990: Frequency–wavenumber spectrum for GATE phase I rainfields. *J. Appl. Meteor.*, **29,** 841–850.

Newton, H. J., 1988: *TIMESLAB: A Time Series Analysis Laboratory.* Wadsworth & Brooks/Cole Publishing Company, 623 pp.

North, G. R., and S. Nakamoto, 1989: Formalism for comparing rain estimation designs. *J. Atmos. Oceanic Technol.*, **6,** 985–992.

——, S. S. P. Shen, and R. B. Upson, 1991: Combining rain gages with satellite measurements for optimal estimates of area–time averaged rain rates. *Water Resour. Res.*, **27,** 2785–2790.

——, ——, and ——, 1993: Sampling errors in rainfall estimates by multiple satellites. *J. Appl. Meteor.*, **32,** 389–410.

——, J. D. Valdes, E. Ha, and S. S. P. Shen, 1994: The ground-truth problem for satellite estimates of rain rate, *J. Atmos. Oceanic Technol.*, in press.